

Article

Concentration, Spatial Distribution, and Source Analysis of Trace Elements in the Yarlung Zangbo River Basin and Its Two Tributaries

Fangjing Xiao , Yuanzhao Zhao, Duo Bu  and Qingying Zhang *

College of Ecological Environment, Tibet University, Lhasa 850000, China; xfj2023@utibet.edu.cn (F.X.); 15617927906@163.com (Y.Z.)

* Correspondence: phudor@vip.163.com (D.B.); zhangqingying@utibet.edu.cn (Q.Z.)

Abstract: The Yarlung Zangbo River (YZR) is the longest plateau river in China and has famous tributaries, the Lhasa River and the Nianchu River. A total of 75 water samples were collected from the Yarlung Zangbo River Basin (YZRB) in this study to investigate the dissolved concentration, spatial distribution, and source of trace elements (Fe, V, Be, Ti, Mo, Se, Cd, Zn, Cu, Ni, Co, Mn, Cr, Ba, Tl, Pb, Hg, As, and Sb). The results indicate that only Cr and Tl contaminate water, while the other trace elements were in an unpolluted state. In addition, correlation analysis showed that there was a highly significant positive correlation between the concentrations of As, Sb, and Mo; there was also a highly significant positive correlation between the concentrations of Fe, Mn, Ti, Pb, Ni, Co, and Ba. The results of Positive Matrix Factorization (PMF) showed that there were four sources of trace elements in the YZRB, including the resuspension and dissolution of sediments (16.283%), agricultural source (11.436%), lithological source (47.418%), and soil-forming rocks (6.374%). Cluster analysis combined with PMF normalized contribution analysis, which showed that the trace elements found in the YZR's mainstream were predominantly influenced by the surrounding rocks composition. Meanwhile, both the discharge of mining wastewater and sediments were marked in the Lhasa River. Additionally, agricultural activities were the chief contributors to the trace elements in the Nianchu River. Furthermore, the entire basin was subjected to the influence of soil-forming rocks. This study comprehensively analyzed and evaluated the physicochemical properties of water, the spatial distribution, and the pollution degree, and performed source analysis of trace elements in the YZRB. This research provides a foundational reference for further investigation of the spatial distribution and origins of trace elements in the rivers of the Qinghai–Tibet Plateau (QTP).

Keywords: Yarlung Zangbo River; trace elements; spatial distribution; pollution degree; source analysis



Citation: Xiao, F.; Zhao, Y.; Bu, D.; Zhang, Q. Concentration, Spatial Distribution, and Source Analysis of Trace Elements in the Yarlung Zangbo River Basin and Its Two Tributaries. *Water* **2023**, *15*, 3558. <https://doi.org/10.3390/w15203558>

Academic Editors: Begoña González and Gene Hall

Received: 26 August 2023

Revised: 7 October 2023

Accepted: 10 October 2023

Published: 12 October 2023



Copyright: © 2023 by the authors. Licensee MDPI, Basel, Switzerland. This article is an open access article distributed under the terms and conditions of the Creative Commons Attribution (CC BY) license (<https://creativecommons.org/licenses/by/4.0/>).

1. Introduction

The Qinghai–Tibet Plateau (QTP), with its status as the “Asia water tower”, is the main water source and ecological barrier in Asia. Being both the most crucial and fragile reservoir of water resources, the inherent significance of this water tower is undeniable and has been widely acknowledged in numerous authoritative studies [1,2]. Generally, the QTP was considered to be the most limited primitive area of human influence, where most of the rivers in Tibet were considered uncontaminated [3]. Nowadays, with the intensification of human activity (such as tourism, mining operations, urban sewage discharge, and arable land), the potential risks caused by trace elements to local ecosystems have gradually become prominent [4].

Heavy metal pollution in the QTP has appeared in different environmental media, especially in some rivers [5]. Although the rivers in the QTP can usually be regarded as primitive rivers, due to the increasing impact of human activity, the concentration of some toxic elements (i.e., Cd and Pb) is higher than the World Health Organization's drinking water guidelines, which poses a risk to human livelihoods in the local and surrounding

areas. Wang et al. stated that some trace elements, such as Cu (13.92 µg/L), As (41.60 µg/L), and Pb (26.69 µg/L) in the lake of Yamdrok–tso Basin were characterized by high dissolved concentration values [6]. Zhang et al. revealed that the significant enrichment of As in Singe Zangbo River water (up to 104 µg/L) was sourced from hot springs and evaporite [7].

Trace elements enter the water through mining wastewater [8], the chemical industry [9], pesticides and fertilizers [10], atmospheric deposition [11], and soil weathering [12]. They are important factors affecting the safety evaluation of the water's ecological environment. Therefore, Fe, V, Be, Ti, Mo, Se, Cd, Zn, Cu, Ni, Co, Mn, Cr, Ba, Tl, Pb, Hg, As, and Sb were used as water quality monitoring indicators to assess the Environmental Quality Standards for Surface Water (GB3838–2002) [13]. To comprehensively understand the impact of trace elements on water quality and health risks, it is usually necessary to classify the sources of trace elements and use a pollution index and health risk index to describe the degree of heavy metal pollution and health hazards. Therefore, studying the water quality status and health risks of the Tibet Plateau is of crucial significance when revealing the potential threats to water security and protecting water resources. The research results of trace elements in the water of the study basin are not comprehensive enough. Therefore, this paper analyzes the spatial distribution characteristics and source analysis of trace elements in different reaches of the Yarlung Zangbo River Basin (YZRB).

The purpose of this study is (1) to reveal the concentration and spatial distribution characteristics of trace elements in the water of the YZRB and its two tributaries; (2) to evaluate the pollution characteristics of trace elements in the watershed; (3) to trace its possible sources and analyze its proportion using the Positive Matrix Factorization (PMF). This comprehensive study thoroughly analyzes and assesses the physicochemical properties, trace element pollution characteristics, spatial distribution patterns, and source apportionment within the YZRB. It unveils the current water environmental quality of the YZRB and serves as a valuable reference for investigating the concentration, distribution characteristics, and sources of various trace elements in rivers across the Tibetan Plateau.

2. Materials and Methods

2.1. Study Area

The study area (28°40′44″ N~29°51′38″ N, 88°51′50″ E~92°45′34″ E) of YZRB is located in the southern part of the Tibet Plateau in China, including the middle of the YZRB and the two tributaries (Lhasa River and Nianchu River), a well-known base for self-evident food production. As shown in Figure 1, a tributary of the Lhasa River is located in the capital city of Tibet (Lhasa), exposed to copper mining and distributions of geothermal resources [14]. The most common pollutants entering the river are Cu and As. In contrast, the other tributary (Nianchu River) is densely populated with facility agriculture [15], indicating that the main source of pollution is agricultural non-point source pollution. Overall, the YZRB exhibits ancient karst geological characteristics [16]. From September to October 2021, water samples ($n = 75$) were collected and presented as Y1–20 (YZR's mainstream), L1–14 (Lhasa River), and N1–41 (Nianchu River). The average altitude of the sampling points reached 3762 m. The basin is also rich in species diversity and is affected by unique high-altitude cold climatic conditions, making it one of the most vulnerable areas in Asia.

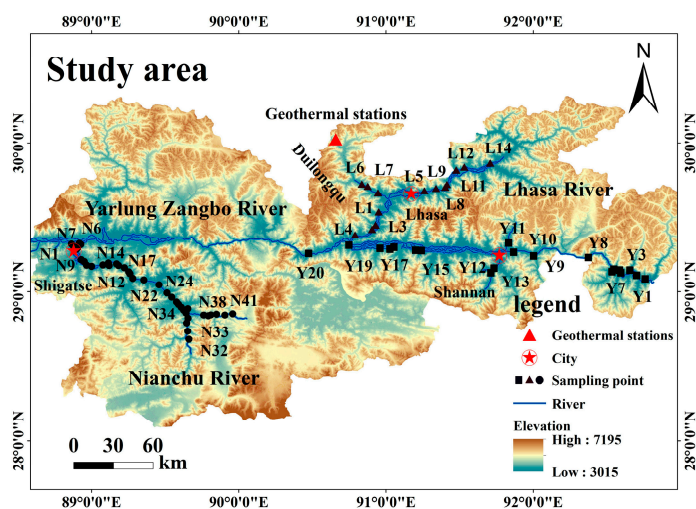


Figure 1. Study area and the geographical location of sampling sites.

2.2. Sample Collection and Analysis

According to the terrain and on-site environment, the spacing between each sampling site is about 2.5–10 km. Specifically, some important sampling sites (Y19, N6) are set after tributary flows into the mainstream and are also fully mixed. By comparison, the control section sampling sites (N7, L4) are set before tributary flows into the mainstream. The collection of water samples is conducted as follows: prior to sampling, the sampling apparatus, containers, and container lids were acid-washed with 10% (*v/v*) high-quality pure nitric acid. Water samples were collected in 500 mL acid-cleaned brown polyethylene bottles, 10 cm below the water surface. After multi-parameter analysis of the water sample on site, the collected sample was filtered through acid-cleaned Millipore filters (25 mm diameter, 0.45 μm mixed cellulose esters membrane). Approximately 15 mL filtered water samples were transferred into polyethylene bottles (pre-acid-washed with 10%, *v/v*, high-quality pure nitric acid) and stored in boxes with ice. After collection, the water samples were transported to the laboratory for trace elements analysis. To determine the field parameters, a portable dissolved oxygen meter (HANNA, HI98193, Rhode Island, Italy) and a portable multi-parameter measuring instrument (Thermo, Eutech PCS Testr 35, Massachusetts, USA) were used to measure the dissolved oxygen (DO), temperature (T), electrical conductivity (EC), pH, total dissolved solids (TDS), and salinity (SAL) in water. In this study, the concentrations of Fe, V, Be, Ti, Mo, Se, Cd, Zn, Cu, Ni, Co, Mn, Cr, Ba, Tl, Pb, and Sb were detected using an inductively coupled plasma mass spectrometer (ICP-MS, PerkinElmer, NexION1000, Waltham, MA, USA). The concentrations of As and Hg were detected via an atomic fluorescence spectrometer (AFS, Beijing Titan, AFS-830, Beijing, China).

2.3. Evaluation of the Contamination

The Nemerow integrated pollution index method is a commonly used and representative method for the evaluation of trace elements in water [17]. It is divided into a single-factor pollution index (P_i) and a multi-factor-integrated pollution index (P_n). The evaluation of P_i can only reflect the pollution status of a single element, while P_n considers the influence of extreme values or prominent maximum values of multiple elements. Multiple trace elements often coexist in water, and the Nemerow-integrated pollution index method can reflect the status of trace element pollution in water and the different contributions various trace elements form in composite pollution. It also screens the main pollutants, which is also one of the common methods for the evaluation of trace element pollution in water.

$$P_i = C_i/S_i \quad (1)$$

$$P_n = \sqrt{\frac{\max(P_i)^2 + \text{ave}(P_i)^2}{2}} \quad (2)$$

Here, C_i is the measured concentration of trace element i ; S_i is the corresponding standard reference concentration, using the standard reference values of the Chinese standard GB3838–2002 [13]. $\max(P_i)$ is the maximum value of the trace element single-factor pollution index, and $\text{ave}(P_i)$ is the average value of the single-factor pollution index of trace elements. The classification of the potential contamination level of trace elements is presented in Table 1 [18].

Table 1. Classification of the potential contamination level of trace elements.

P_i	Pollution Grading	P_n	Pollution Grading
$P_i \leq 1$	no pollution	$P_n \leq 0.7$	clean level
$1 < P_i \leq 2$	low pollution	$0.7 < P_n \leq 1$	precaution level
$2 < P_i \leq 3$	moderate pollution	$1 < P_n \leq 2$	light pollution level
$3 < P_i \leq 5$	strong pollution	$2 < P_n \leq 3$	moderate level
$P_i > 5$	very strong pollution	$P_n > 3$	heavy pollution level

2.4. Source Apportionment

PMF is a method for the quantitative analysis of pollution sources using sample composition [19]; it decomposes the pollutant concentration matrix X into a source factor contribution matrix G , factor distribution matrix F , and residual matrix E , which are then calculated as follows:

$$X_{ij} = \sum_{k=1}^p G_{ik}F_{kj} + E_{ij} \quad (3)$$

Here, X_{ij} is the measurement matrix of the j th trace element in the i sample; G_{ik} is the contribution matrix of the k th source factor of the i sample; F_{kj} is the distribution matrix of the j th trace element in the k th source factor; and E_{ij} is the residual value of the j th trace element in the i sample. The cumulative residual Q -value can be minimized for factor contribution and distribution using the PMF model.

$$Q = \sum_{i=1}^n \sum_{j=1}^m \left[\frac{X_{ij} - \sum_{k=1}^p G_{ik}F_{kj}}{U_{ij}} \right]^2 \quad (4)$$

Here, PMF is required to import uncertainty data before it is run. If the trace element concentration does not exceed the species-specific method detection limit (MDL value), then the value of uncertainty (U_{nc}) is equal to 5/6 MDL; otherwise, the uncertainty U_{nc} is calculated using Equation (6):

$$\text{If } X_{ij} \leq \text{MDL} \quad U_{nc} = 5/6 \times \text{MDL} \quad (5)$$

$$U_{nc} = \sqrt{(\text{Error Fraction} \times \text{concentration})^2 + (0.5 \times \text{MDL})^2} \quad (6)$$

Here, X_{ij} is the measurement matrix of the j th trace element in i samples, and the error fraction is the relative standard deviation of trace element concentrations.

2.5. Statistical Analysis

The sampling layout was carried out using statistics and ArcGIS 10.7, and the Kriging interpolation method revealed variability and spatial and temporal distribution characteristics of the trace elements. The Nemerow-integrated pollution index was used to analyze the contamination degree of the trace elements. PMF was used to discuss the correlation, source number, and contribution rate of trace elements in the YZRB and its two tributaries. PMF source apportionment was conducted using the matrix factorization model of EPA

PMF 5.0. IBM SPSS Statistics 25 and Origin Pro 2021 software were used for systematic cluster analysis.

3. Results and Discussion

3.1. Physical and Chemical Parameters

Conventional physicochemical parameters characterize the basic water environment characteristics of YZRB. The conventional physicochemical parameters of water mainly include DO, T, EC, pH, TDS, and SAL. The average pH value of the basin was ranked as Nianchu River (8.92) > Lhasa River (8.42) > YZR's mainstream (7.32). Due to the fact that sampling was conducted during the warm season, the water temperature and DO values in the basin were relatively high at 14.7 °C and 4.61 mg/L, respectively. In addition, EC (mean 443 $\mu\text{S}/\text{cm}$), SAL (mean 214 mg/L), and TDS (mean 313 mg/L) in the YZRB were higher than the average value of the world river [20], which is consistent with the strong erosion of the plateau basin and the lithological composition of carbonate rocks. In addition, EC, TDS, and SAL showed a significant positive correlation ($p < 0.01$).

3.2. Evaluation of the Contamination

For comparison, the average concentrations of trace elements in the YZRB reported in the literature [3,21–26] were listed, as shown in Table 2. The trace elements (average concentration) measured in this work were found not to be significantly different from those reported in the literature, and the concentration levels were observed to be at almost the same level. Moreover, the reliability of the original data was tested using a standard solution, and it was found that the accuracy of the elements was between 74.5% (V) and 107% (Pb), indicating that the determination method is accurate and reliable.

Based on the concentration levels detected using trace elements, the single-factor (P_i) and multi-factor-integrated pollution index (P_n) of trace elements were evaluated. Among all the surveyed elements, elements with a P_i value less than one exhibited no pollution; therefore, these elements are not discussed. As shown in Figure 2a, only five trace elements (Cr, Cu, Fe, Tl, and Ti) have a maximum P_i value greater than one, indicating low pollution. Overall, the evaluation results of the P_i value indicate that YZRB was on a clean level; however, some sampling sites (2–7) showed outliers. Similar to the P_n value presented in Figure 2b, the elements of Cr and Tl had P_n values greater than 0.7, while the order of pollution degree was Tl (1.03) > Cr (0.86). Cr belongs to the precaution level; Tl belongs to the light pollution level. Specifically, the distribution of sampling sites with P_n values higher than 0.7 were N10, N13, N25, and N26 for Cr, N21 and N31 for Tl, respectively. The results indicate the presence of Cr and Tl contamination in the Nianchu River Basin, which could be associated with the region's agriculture and geological composition [27,28]. Compared with the evaluation results of the water quality pollution status for each monitoring region of the YZRB using P_i , P_n comprehensively considered the more seriously polluted indicators, which reflected the degree of water pollution, and also considered the average value of P_i , supplementing the shortcomings of P_i . Therefore, P_n is more comprehensive than P_i for water quality evaluation.

Table 2. Comparison of average concentrations of trace elements in the YZRB (unit: $\mu\text{g/L}$).

Trace Elements	Fe	V	Be	Ti	Mo	Se	Cd	Zn	Cu	Ni	Co	Mn	Cr	Ba	Tl	Pb	Hg	As	Sb	References
Min	4.5	<5	0.03	0.4	0.096	<0.25	0.06	0.8	0.14	0.8	0.046	0.06	0.09	1	<0.01	0.007	<0.4	0.12	0.078	This study
Max	700	<5	1.3	150	4.2	0.29	0.22	29	28	9.9	1.35	32.9	55	92	0.2	1.1	<0.4	28	3.5	
Mean	101.107	<5	0.143	9.711	1.001	<0.25	0.074	2.507	2.046	2.888	0.249	3.261	4.903	16.851	0.043	0.177	<0.4	2.335	0.639	
Mean	14.925	–	–	0.938	1.518	–	–	–	–	–	–	16.829	–	–	–	–	–	–	–	[21]
Mean	16.628	–	–	0.621	1.673	–	–	–	–	–	–	4.12	–	–	–	–	–	24.48	–	[22]
Mean	–	–	–	–	1.4	–	3.6	20.5	1.9	2.8	–	30.7	2.8	15.3	–	15.8	–	–	4.3	[3]
Mean	–	–	–	7.8	1.2	–	1	9.8	1.4	–	–	12.8	2.7	12	<0.007	5.6	3.225	10.5	3.4	[23]
Mean	20.592	–	–	0.368	0.821	–	0.088	10.8	1.124	–	–	54.86	0.128	43.285	0.014	0.557	0.023	0.862	–	[24]
Mean	30	–	–	7.51	1.83	0.05	0.04	0.53	0.76	2.4	0.37	5.43	4.01	–	–	0.13	0.03	12.2	–	[25]
World Mean	66	–	0.009	0.489	0.42	0.07	0.08	0.6	1.48	0.801	0.148	34	0.7	23	–	0.079	–	0.62	0.07	[26]

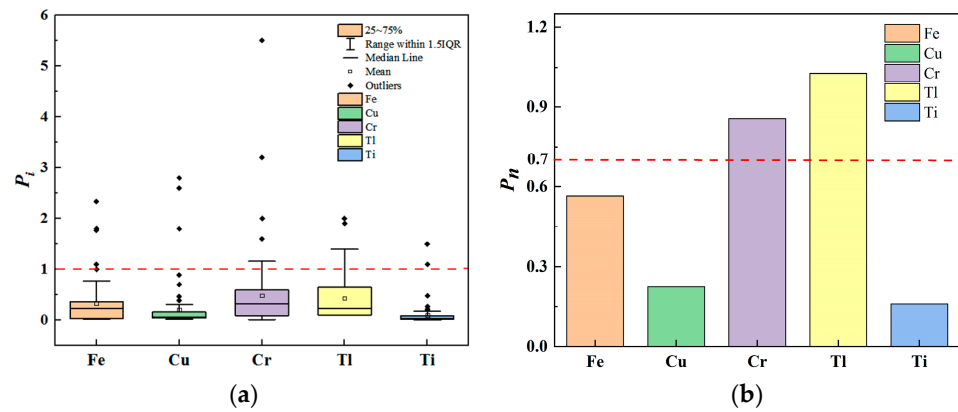


Figure 2. Pollution index of trace elements in the YZRB: (a) Single-factor index (P_i); (b) multi-factor-integrated pollution index (P_n).

3.3. Spatial Distribution

To present the spatial distribution characteristics of each trace element more clearly, the geographic information system (GIS) method [29,30] was used to perform spatial interpolation analysis on the 16 trace elements, and the spatial distribution graph is shown in Figure 3. Se, Hg, and V were not shown due to weak variability. As, Ba, Mo, and Sb were mainly distributed in Duilongqu (right tributary of the Lhasa River); Zn and Cu were mainly distributed in the Lhasa River; Fe, Mn, Ti, Co, Cr, Tl, and Be were mainly distributed in the Nianchu River Basin. The spatial distribution of Zn and Cu was consistent with the distribution of mines. The distribution of mining areas was mainly concentrated in Duilongdeqing County and Mozhugongka County in Lhasa City [31]. The spatial distribution of As was consistent with the distribution of geothermal resources in the Lhasa River Basin [32,33]. Due to the input of geothermal water, the concentration of As in the Lhasa River Basin was high [34,35]. The trace elements of Mn, Fe, Ti, Pb, and Co were speculated to be weathering of soils input around the river [21]. Cr and Ti were mainly distributed in the Nianchu River Basin, possibly owing to agricultural activities [36,37]. Spatial distribution provides more intuitive assistance when analyzing the source of elements.

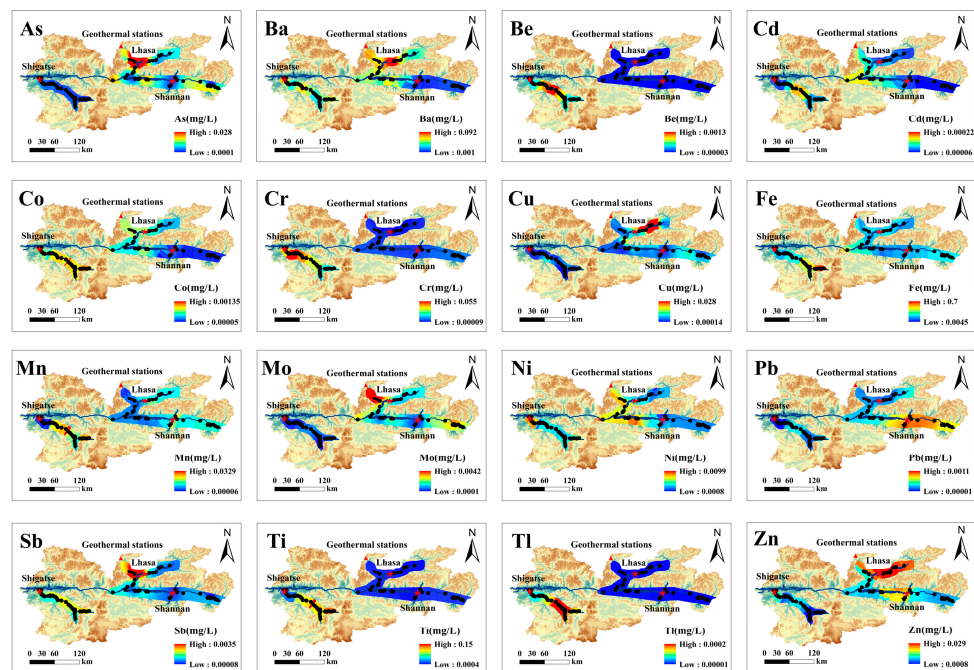


Figure 3. Spatial distribution of trace elements.

3.4. Source Apportionment

3.4.1. Correlation Analysis

Analyzing correlations between trace elements can provide a better understanding of their affinity, and a strong affinity between them indicates that these sources are likely to be the same [38,39]. Due to the concentrations of V and Hg being below the detection limits (0.005 and 0.0004 mg/L, correspondingly), the correlation between Hg, V, and other elements was not discussed. As presented in Figure 4a, there were significant correlations among As, Sb, and Mo ($p < 0.01$); Fe, Mn, Ti, Pb, Ni, Co, and Ba ($p < 0.01$), implying their affinity. Pearson correlation analysis can assist PMF in traceability. Although correlation analysis can demonstrate the affinity between elements, it cannot reveal source contributions. Therefore, it is necessary to use the PMF model for source contribution analysis.

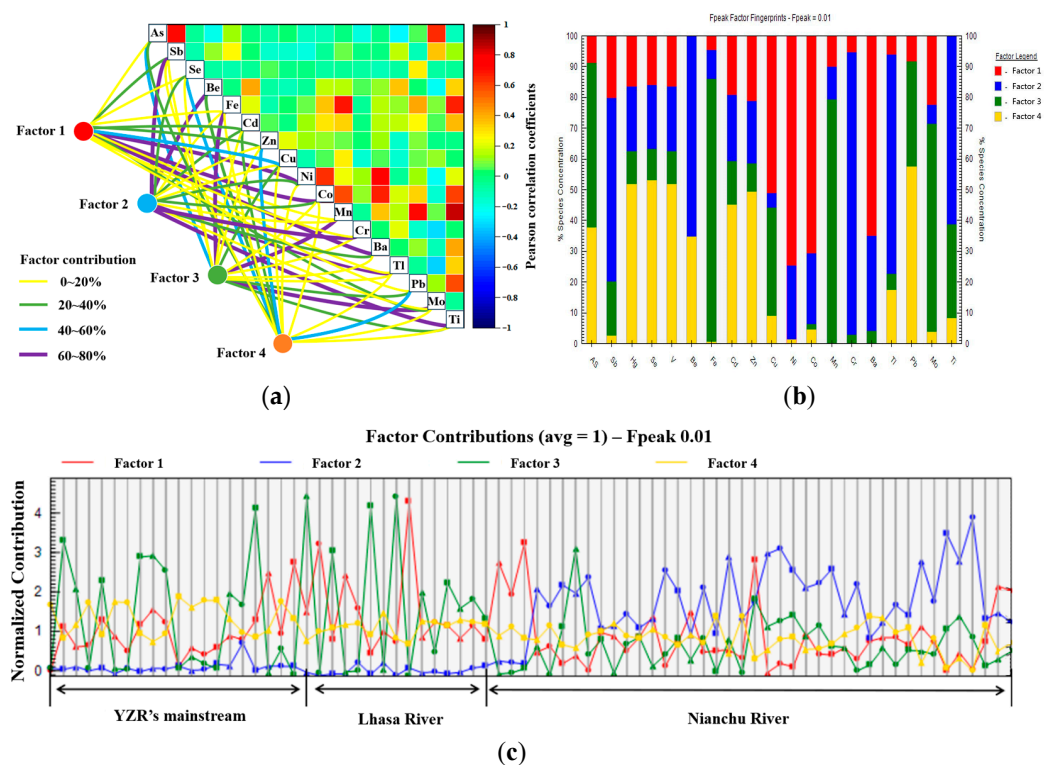


Figure 4. The sources of trace elements were analyzed via PMF: (a) Pearson correlation coefficient; (b) factor analysis and contribution rate; (c) the normalized contributions.

3.4.2. Source Analysis of PMF Model

Through PMF model analysis, four contribution factors were found in the YZRB. Clearly, Figure 4b delineates the contribution concentration and contribution ratio of various trace elements as factors. Generally, a high contribution concentration that simultaneously meets a high contribution ratio can be identified as the dominant contribution factor [40,41].

Factor 1 (F1) was mainly loaded on Cu, Ni, Co, Zn, and Ba. Based on spatial distribution, there are copper mines distributed upstream of the Lhasa River [42,43]; therefore, the source of Cu and Zn is the mining wastewater discharge. Also, Ni, Co, and Ba are released into the aquatic environment as a result of the resuspension and dissolution of river sediments [44–46]. Therefore, F1 can be attributed to the source of mining wastewater and sediments (16.283%). Factor 2 was dominated by Cr, Sb, and Ti. Previous studies have shown that the concentration of Cr in fertilizers and pesticides is generally high (11.5–94.6 mg/kg) [47]. Based on the previous spatial distribution results, Cr had high concentrations in the Shigatse greenhouse area. In addition, certain agricultural activities also use titanium-containing compounds [48,49]. Therefore, F2 can be attributed to the source of agricultural activities (11.436%). Factor 3 was dominated by Fe, As, Mn, and

Mo. Interestingly, both As and Mo elements exhibited a high value of distribution in the Duilongqu Basin, where geothermal resources are widely distributed. Considering that YZRB is an ancient karst region, with huge potential for Fe and Mn deposits [16,50–52], F3 could be identified as a lithological source and geothermal wastewater (47.418%). Factor 4 (F4) was mainly loaded on Hg, Se, V, and Zn. As mentioned above, the spatial distribution for Se, Hg, and V showed weak variability, with detection concentrations appearing relatively low. Thus, F4 was predominantly characterized by Zn. Zn mainly exhibits a high-value distribution in the Lhasa River Basin, and this overall regional variation was not significant when manifested by the weathering of soils [53]. Therefore, F4 was primarily from soil-forming rocks (6.374%).

Figure 4c presents the normalized contribution source analysis in each watershed. The results show that the trace elements found in the YZRB were predominantly influenced by the surrounding rock composition (F3 and F4). Meanwhile, the Lhasa River water environment marked both the discharge of mining/geothermal wastewater (F1 and F3). Additionally, agricultural activities (F2) were the chief contributors to trace elements in the Nianchu River.

3.4.3. Cluster Analysis

To visualize the origins of trace elements at each sampling point, cluster analysis was conducted [54]. The diagrams of clustering analysis yielded for the sampling sites are shown in Figure 5.

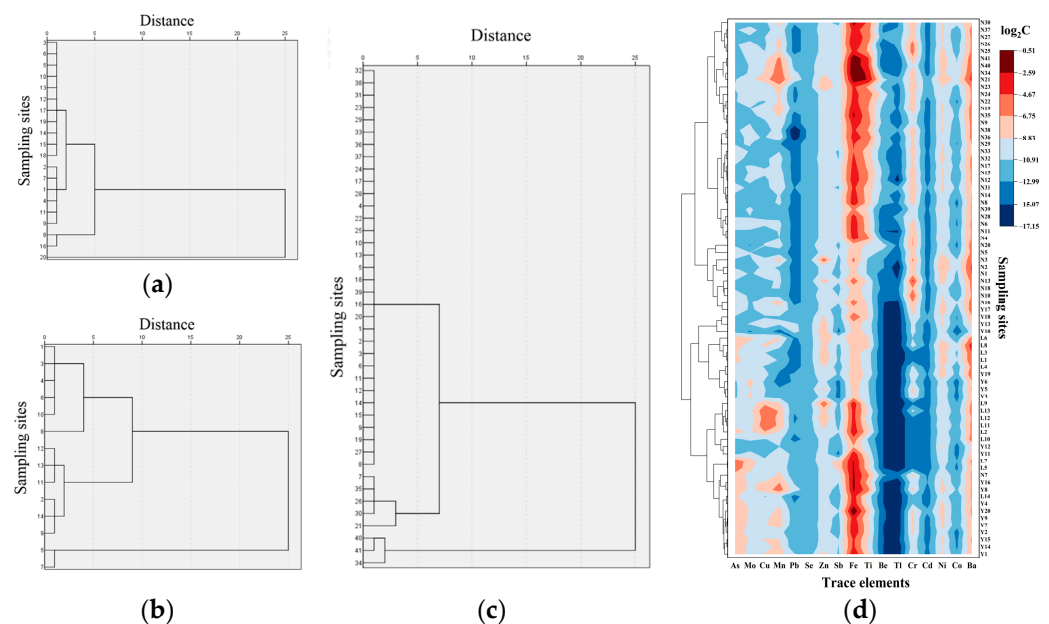


Figure 5. Cluster analysis of sampling sites in the YZRB: (a) YZR’s mainstream; (b) Lhasa River; (c) Nianchu River; (d) clustering heat map of the whole sampling sites in the YZRB. C represents the concentration of trace elements (unit: mg/L).

In Figure 5a, the sampling sites in the YZR’s mainstream can be divided into three categories. There are seventeen sampling sites (Y1–7, Y7–15, and Y17–19), two sampling sites (Y8 and Y16), and one sampling site (Y20) in these three categories, respectively. The sampling sites with the highest proportion were all least affected by human activities. The sampling sites of Y8 and Y16 were located near the highway and were greatly affected by traffic sources. At sampling point Y20, a substantial sediment deposit accumulated on the riverbed, leading to the re-release of Fe from the sediment. Therefore, the main source of the YZR’s mainstream is the surrounding rock composition.

In Figure 5b, the sampling sites in the Lhasa River can be divided into three categories. There are six sampling sites (L1, L3, L4, L6, L8, and L10) in the first category. These sampling

sites are located downstream of Lhasa city and are affected by the input of production and domestic sewage. There are six sampling points (L2, L9, and L11–14) in the second category. Significantly, sampling sites from L11 to L14 were located downstream of the mining area (Mozhugongka County). Mining wastewater input was the most important source. The third type includes two sampling sites (L5 and L7), both of which were downstream of Duilongqu, where geothermal resources were widely distributed. Therefore, geothermal wastewater from Yangbajing produced a significant effect [55]. In conclusion, the main source of the Lhasa River was the discharge of mining and geothermal wastewater.

In Figure 5c, the sampling sites of Nianchu River are divided into three categories. There are 33 sampling sites in the first category, N1–6, N8–20, N22–25, N27–29, N31–33, and N36–39. Most of these sites are surrounded by greenhouses. Based on the pollution assessment results, the P_i values of Cr at these sites are significantly high. Thus, the main sources of pollution at these sampling sites are agricultural activities.

In Figure 5d, a clustering heat map of sampling points in the whole YZRB is shown. It can be seen from the color that the concentration of Fe is higher than that of other trace elements in the whole basin, which is consistent with the factor distribution and contribution rate plot of PMF.

4. Conclusions

In conclusion, this study investigated the concentration levels, spatial distribution, and sources of 19 trace elements in the YZRB. Through the evaluation of the Nemerow pollution index, the YZRB was considered to be in an unpolluted state with limited human impact. Due to their high P_i values, five trace elements (Cr, Cu, Fe, Tl, and Ti) need to be continuously studied in future research. The spatial distribution of Cu and Zn is consistent with the distribution of mines, while the spatial distribution of As is consistent with the distribution of geothermal resources. Cr is mainly distributed in the Nianchu River Basin, and Fe is uniformly distributed throughout the basin. The use of PMF to analyze trace element sources, conduct correlation analysis, and perform cluster analysis is an innovative way to assist with its traceability. Cluster analysis combined with PMF source analysis showed that the trace elements found in the YZRB were predominantly influenced by the lithological composition of host rocks, with the Lhasa River showing the discharge of mining and geothermal wastewater and the Nianchu River being affected by agricultural activities. Furthermore, the entire basin was subjected to the influence of soil-forming rocks. This study comprehensively examines trace element spatial characteristics in the YZRB, utilizing surface, line, and point perspectives. It employs Kriging for surface analysis to study trace element distribution. Shifting to a line approach, it conducts a comparative analysis of contributions from four sources in three river sections, using normalized contribution for precise source tracing. Finally, at the point level, cluster analysis is employed to understand factors behind trace element concentration outliers at various sampling points. This study seamlessly transitions from a surface to line and point perspective and is expected to provide a foundational reference for further research on the spatial distribution and sources of trace elements in rivers on the QTP.

Author Contributions: Conceptualization, F.X. and Y.Z.; methodology, F.X.; software, F.X.; validation, F.X., Y.Z. and Q.Z.; formal analysis, F.X.; investigation, Y.Z.; resources, D.B.; data curation, F.X.; writing—original draft preparation, F.X.; writing—review and editing, F.X. and Q.Z.; visualization, F.X.; supervision, Q.Z.; project administration, D.B.; funding acquisition, D.B. All authors have read and agreed to the published version of the manuscript.

Funding: This research was funded by the Second Comprehensive Scientific Investigation Project of Qinghai-Tibet Plateau (No.2019QZKK0603), the National Natural Science Foundation of China (No.22266032, No.41967059), State Key Laboratory of Environmental Chemistry and Ecotoxicology, Research Center for Eco-Environmental Sciences, Chinese Academy of Sciences (No.KF2021-05), Central Financial Support Special Funds for Local Colleges and Universities ([2023] No.1).

Data Availability Statement: The datasets used and analyzed during the current study are available from the corresponding author on reasonable request.

Conflicts of Interest: The authors declare no conflict of interest.

References

- Immerzeel, W.W.; Lutz, A.F.; Andrade, M.; Bahl, A.; Biemans, H.; Bolch, T.; Hyde, S.; Brumby, S.; Davies, B.J.; Elmore, A.C.; et al. Importance and vulnerability of the world's water towers. *Nature* **2020**, *577*, 364–369. [CrossRef]
- Li, Y.; Han, F.; Zhou, H. Assessment of terrestrial ecosystem sensitivity and vulnerability in Tibet. *J. Resour. Ecol.* **2017**, *8*, 526–537.
- Qu, B.; Zhang, Y.; Kang, S.; Sillanpää, M. Water chemistry of the southern Tibetan Plateau: An assessment of the Yarlung Tsangpo river basin. *Environ. Earth Sci.* **2017**, *76*, 74. [CrossRef]
- Wu, J.; Duan, D.; Lu, J.; Luo, Y.; Wen, X.; Guo, X.; Boman, B.J. Inorganic pollution around the Qinghai-Tibet Plateau: An overview of the current observations. *Sci. Total Environ.* **2016**, *550*, 628–636. [CrossRef]
- Dutta, S.; Dutta, P.; Devi, U.; Sarmaa, K.P. Distribution and pollution status of metals in some water bodies of mid-Brahmaputra valley. *Desalin. Water Treat.* **2017**, *65*, 215–223. [CrossRef]
- Wang, C.; Zhou, H.; Kuang, X.; Hao, Y.; Shan, J.; Chen, J.; Li, L.; Feng, Y.; Zou, Y.; Zheng, Y. Water quality and health risk assessment of the water bodies in the Yamdrok-tso basin, southern Tibetan Plateau. *J. Environ. Manag.* **2021**, *300*, 113740. [CrossRef]
- Zheng, T.; Deng, Y.; Lin, H.; Xie, Y.; Pei, X. Hydrogeochemical controls on As and B enrichment in the aqueous environment from the Western Tibetan Plateau: A case study from the Singe Tsangpo River Basin. *Sci. Total Environ.* **2022**, *817*, 152978. [CrossRef]
- Huang, X.; Sillanpää, M.; Gjessing, E.T.; Peräniemi, S.; Vogt, R.D. Environmental impact of mining activities on the surface water quality in Tibet: Gyama valley. *Sci. Total Environ.* **2010**, *408*, 4177–4184. [CrossRef]
- Kara, G.T.; Kara, M.; Bayram, A.; Gündüz, O. Assessment of seasonal and spatial variations of physicochemical parameters and trace elements along a heavily polluted effluent-dominated stream. *Environ. Monit. Assess.* **2017**, *189*, 585. [CrossRef]
- Zhan, S.; Wu, J.; Jin, M. Hydrochemical characteristics, trace element sources, and health risk assessment of surface waters in the Amu Darya Basin of Uzbekistan, arid Central Asia. *Environ. Sci. Pollut. Res.* **2022**, *29*, 5269–5281. [CrossRef]
- Cong, Z.; Kang, S.; Zhang, Y.; Li, X. Atmospheric wet deposition of trace elements to central Tibetan Plateau. *Appl. Geochem.* **2010**, *25*, 1415–1421. [CrossRef]
- Jin, Z.; You, C.; Yu, T.; Wang, B. Elemental distribution in the topsoil of the Lake Qinghai catchment, NE Tibetan Plateau, and the implications for weathering in semi-arid areas. *J. Geochem. Explor.* **2015**, *152*, 1–9.
- State Environmental Protection Administration of the People's Republic of China. *Environmental Quality Standards for Surface Water*; State Environmental Protection Administration of the People's Republic of China: Beijing, China, 2002. Available online: https://www.mee.gov.cn/ywgz/fgbz/bz/bzwb/shjbh/shjzlbz/200206/t20020601_66497.shtml (accessed on 26 May 2023).
- Xia, Z.; Zhang, J.; Yan, Y.; Zhang, W.; Zhao, Z. Heavy metals in suspended particulate matter in the Yarlung Tsangpo River, Southwest China. *GeoSyst. Geoenviron.* **2022**, 100160. [CrossRef]
- Shi, D.; Tan, H.; Chen, X.; Rao, W.; Issombo, H.E.; Basang, R. Temporal and spatial variations of runoff composition revealed by isotopic signals in Nianchu River catchment, Tibet. *J. Hydrol. Environ. Res.* **2021**, *37*, 1–12. [CrossRef]
- Zhou, X.; Ao, Y.; Jiang, X.; Yang, S.; Hu, Y.; Wang, X.; Zhang, J. Water use efficiency of China's karst ecosystems: The effect of different ecohydrological and climatic factors. *Sci. Total Environ.* **2023**, *905*, 167069. [CrossRef]
- Su, K.; Wang, Q.; Li, L.; Cao, R.; Xi, Y. Water quality assessment of Lugu Lake based on Nemerow pollution index method. *Sci. Rep.* **2022**, *12*, 13613. [CrossRef]
- Belle, G.; Schoeman, Y.; Oberholster, P. Potential toxic-element pollution in surface water and its implications for aquatic and human health: Source-pathway-receptor model. *Water* **2023**, *15*, 3100. [CrossRef]
- Paatero, P.; Tapper, U. Positive matrix factorization: A non-negative factor model with optimal utilization of error estimates of data values. *Environmetrics* **2010**, *5*, 111–126. [CrossRef]
- Wetzel, R.G. Lake and river ecosystems. In *Limnology*; Academic Press: San Diego, CA, USA, 2002.
- Huang, X.; Sillanpää, M.; Gjessing, E.T.; Vogt, R.D. Water quality in the Tibetan Plateau: Major ions and trace elements in the headwaters of four major Asian rivers. *Sci. Total Environ.* **2009**, *407*, 6242–6254. [CrossRef]
- Huang, X.; Sillanpää, M.; Gjessing, E.T.; Peräniemi, S.; Vogt, R.D. Water quality in the southern Tibetan Plateau: Chemical evaluation of the Yarlung Tsangpo (Brahmaputra). *River Res. Appl.* **2011**, *27*, 113–121. [CrossRef]
- Qu, B.; Zhang, Y.; Kang, S.; Sillanpää, M. Water quality in the Tibetan Plateau: Major ions and trace elements in rivers of the "Water Tower of Asia". *Sci. Total Environ.* **2019**, *649*, 571–581. [CrossRef]
- Wu, J.; Zhao, Z.; Meng, J.; Zhou, T. Analysis on water quality of the Tibetan Plateau based on the major ions and trace elements in the Niyang River Basin. *Appl. Ecol. Environ. Res.* **2020**, *18*, 3729–3740. [CrossRef]
- Liu, J.; Guo, H. Hydrochemical characteristics and ion source analysis of the Yarlung Tsangpo River Basin. *Water* **2023**, *15*, 537. [CrossRef]
- Gaillardet, J.; Viers, J.; Dupré, B. Trace elements in river waters. *Treatise Geochem.* **2003**, *5*, 225–272.
- Du, M.; Zhang, Q.; Ren, P.; Gao, S.; Bu, D. Distribution of soil heavy metals and ecological risk assessment of agricultural land in the Nianchu River Basin, Tibet. *J. Environ. Eng. Technol.* **2022**, *12*, 1618–1625.

28. Guo, J.; Cao, Y.; Luo, Z.; Fang, H.; Chen, Z.; Wang, D.; Xu, F.; Yan, C. Distribution, fractions, and potential release of thallium in acidic soils nearby a waste copper mining site from southern China. *Environ. Sci. Pollut. Res.* **2018**, *25*, 17980–17988. [CrossRef]
29. Madadzada, A.I.; Badawy, W.M.; Hajiyeva, S.R.; Veliyeva, Z.T.; Hajiyev, O.B.; Shvetsova, M.S.; Frontasyeva, M.V. Assessment of atmospheric deposition of major and trace elements using neutron activation analysis and GIS technology: Baku-Azerbaijan. *Microchem. J.* **2017**, *147*, 605–614. [CrossRef]
30. Li, F.; Qiu, Z.; Zhang, J.; Liu, C.; Cai, Y.; Xiao, M. Spatial distribution and fuzzy health risk assessment of trace elements in surface water from Honghu Lake. *Int. J. Environ. Res. Public Health* **2017**, *14*, 1011. [CrossRef]
31. Bu, D.; Xu, Z.; Wu, J.; Li, M.; Dan, Z.; De, J. Study on the impact of mineral processing plant on environment in Lhasa river catchments. *J. Tibet Univ.* **2009**, *24*, 33–38.
32. Zhang, Y.F.; Tan, H.B.; Zhang, W.J.; Huang, J.Z.; Zhang, Q. A new geochemical perspective on hydrochemical evolution of the Tibetan geothermal system. *Geochem. Int.* **2015**, *53*, 1090–1106. [CrossRef]
33. Li, C.; Kang, S.; Chen, P.; Zhang, Q.; Mi, J.; Gao, S.; Sillanpää, M. Geothermal spring causes arsenic contamination in river waters of the southern Tibetan Plateau, China. *Environ. Earth Sci.* **2014**, *71*, 4143–4148. [CrossRef]
34. Guo, Q.; He, T.; Wu, Q.; Liu, M. Constraints of major ions and arsenic on the geological genesis of geothermal water: Insight from a comparison between Xiong'an and Yangbajain, two hydrothermal systems in China. *Appl. Geochem.* **2020**, *117*, 104589. [CrossRef]
35. Zhang, J.; Yan, Y.; Zhao, Z.; Li, X.; Guo, J.; Ding, H.; Cui, L.; Meng, J.; Liu, C. Spatial and seasonal variations of dissolved arsenic in the Yarlung Tsangpo River, southern Tibetan Plateau. *Sci. Total Environ.* **2021**, *760*, 143416. [CrossRef] [PubMed]
36. Xing, W.; Wei, L.; Ma, W.; Li, J.; Liu, X.; Hu, J.; Wang, X. Geochemistry and sources apportionment of major ions and dissolved heavy metals in a small watershed on the Tibetan Plateau. *Water* **2022**, *14*, 3856. [CrossRef]
37. Nguyen, N.T.T.; Nguyen, L.M.; Nguyen, T.T.T.; Liew, R.K.; Nguyen, D.T.C.; Tran, T.V. Recent advances on botanical biosynthesis of nanoparticles for catalytic, water treatment and agricultural applications: A review. *Sci. Total Environ.* **2022**, *827*, 154160. [CrossRef] [PubMed]
38. Li, S.; Zhang, Q. Spatial characterization of dissolved trace elements and heavy metals in the upper Han River (China) using multivariate statistical techniques. *J. Hazard. Mater.* **2010**, *176*, 579–588. [CrossRef] [PubMed]
39. Leonardo, R.D.; Adelfio, G.; Bellanca, A.; Chiodi, M.; Mazzola, S. Analysis and assessment of trace element contamination in offshore sediments of the Augusta Bay (SE Sicily): A multivariate statistical approach based on canonical correlation analysis and mixture density estimation approach. *J. Sea Res.* **2014**, *85*, 428–442. [CrossRef]
40. Pekey, H.; Doğan, G. Application of positive matrix factorisation for the source apportionment of heavy metals in sediments: A comparison with a previous factor analysis study. *Microchem. J.* **2013**, *106*, 233–237. [CrossRef]
41. Comero, S.; Vaccaro, S.; Locoro, G.; Capitani, L.D.; Gawlik, B.M. Characterization of the Danube River sediments using the PMF multivariate approach. *Chemosphere* **2014**, *95*, 329–335. [CrossRef] [PubMed]
42. Zeng, Y.; Chen, J.; Xu, J.; Lei, M.; Xiong, Q. Origin of Miocene Cu-bearing porphyries in the Zhunuo region of the southern Lhasa subterranean: Constraints from geochronology and geochemistry. *Gondwana Res.* **2017**, *41*, 51–64. [CrossRef]
43. Zheng, W.; Tang, J.; Zhong, K.; Ying, L.; Leng, Q.; Ding, S.; Lin, B. Geology of the Jiama porphyry copper-polymetallic system, Lhasa Region, China. *Ore Geol. Rev.* **2016**, *74*, 151–169. [CrossRef]
44. Wang, K.; Zhang, L.; Jiang, X.; Zhao, L.; Wang, S. Determination of background value and potential ecological risk of heavy metals in sediments of a deep Plateau Lake. *Res. Environ. Sci.* **2018**, *31*, 2124–2132.
45. Bai, J.; Li, C.; Kang, S.; Chen, P.; Wang, J. Chemical speciation and risk assessment of heavy metals in the middle part of Yarlung Zangbo surface sediments. *Environ. Sci.* **2014**, *5*, 3346–3351.
46. Dupré, B.; Gaillardet, J.; Rousseau, D.; Allègre, C.J. Major and trace elements of river-borne material: The Congo Basin. *Geochim. Cosmochim. Acta* **1996**, *60*, 1301–1321. [CrossRef]
47. Su, J. The Conventional Pesticide Products Cr, Pb, Cd, As, Hg Heavy Metal Analysis in Gan Su Province. Master's Thesis, Lanzhou University, Lanzhou, China, 2018.
48. Vidmar, J.; Zuliani, T.; Milačič, R.; Ščančar, J. Following the occurrence and origin of titanium dioxide nanoparticles in the Sava River by single particle ICP-MS. *Water* **2022**, *14*, 959. [CrossRef]
49. Rodríguez-González, V.; Terashima, C.; Fujishima, A. Applications of photocatalytic titanium dioxide-based nanomaterials in sustainable agriculture. *J. Photochem. Photobiol. C Photochem. Rev.* **2019**, *40*, 49–67. [CrossRef]
50. Ma, J.; Li, X.; Zhang, C.; Fu, C.; Xie, X.; Wang, X.; Li, X.; Zhang, D.; Bai, Z.; Wang, Z. Recharge source, mode and development potential of typical tectonic karst groundwater in the eastern Qinghai-Xizang Plateau. *Geol. China* **2022**, 1–20. Available online: <http://kns.cnki.net/kcms/detail/11.1167.P.20220822.1417.016.html> (accessed on 1 May 2023).
51. Pu, T.; Kong, Y.; Kang, S.; Shi, X.; Zhang, G.; Wang, S.; Cao, B.; Wang, K.; Hua, H.; Chen, P. New insights into trace elements in the water cycle of a karst-dominated glacierized region, southeast Tibetan Plateau. *Sci. Total Environ.* **2021**, *751*, 141725. [CrossRef]
52. Wen, Y.; Li, W.; Yang, Z.; Zhang, Q.; Ji, J. Enrichment and source identification of Cd and other heavy metals in soils with high geochemical background in the karst region, Southwestern China. *Chemosphere* **2020**, *245*, 125620. [CrossRef] [PubMed]
53. Pan, Y.; Chen, M.; Wang, X.; Chen, Y.; Dong, K. Ecological risk assessment and source analysis of heavy metals in the soils of a lead-zinc mining watershed area. *Water* **2023**, *15*, 113. [CrossRef]

54. Hussain, M.; Ahmed, S.M.; Abderrahman, W. Cluster analysis and quality assessment of logged water at an irrigation project, eastern Saudi Arabia. *J. Environ. Manag.* **2008**, *86*, 297–307. [[CrossRef](#)] [[PubMed](#)]
55. Wang, Y.; Li, L.; Wen, H.; Hao, Y. Geochemical evidence for the nonexistence of supercritical geothermal fluids at the Yangbajing geothermal field, southern Tibet. *J. Hydrol.* **2022**, *604*, 127243. [[CrossRef](#)]

Disclaimer/Publisher's Note: The statements, opinions and data contained in all publications are solely those of the individual author(s) and contributor(s) and not of MDPI and/or the editor(s). MDPI and/or the editor(s) disclaim responsibility for any injury to people or property resulting from any ideas, methods, instructions or products referred to in the content.